

The C/O ratio of He-accreting carbon-oxygen white dwarfs and type Ia supernovae

Xiao Cui (崔晓), Bo Wang (王博), Cheng-Yuan Wu (吴程远), Xiang-Cun Meng (孟祥存) and Zhan-Wen Han (韩占文)

Yunnan Observatories, Chinese Academy of Sciences, Kunming 650216, China; cx@ynao.ac.cn,
zhanwenhan@ynao.ac.cn

Key Laboratory for the Structure and Evolution of Celestial Objects, Chinese Academy of Sciences, Kunming 650216, China

University of the Chinese Academy of Sciences, Beijing 100049, China

Received 2019 May 25; accepted 2019 July 29

Abstract Type Ia supernovae (SNe Ia) are thermonuclear explosions of carbon-oxygen white dwarfs (CO WDs), and are believed to be excellent cosmological distance indicators due to their high luminosity and remarkable uniformity. However, there exists a diversity among SNe Ia, and a poor understanding of the diversity hampers the improvement of the accuracy of cosmological distance measurements. The variations of the ratios of carbon to oxygen (C/O) of WDs at explosion are suggested to contribute to the diversity. In the canonical model of SNe Ia, a CO WD accretes matter from its companion and increases its mass till the Chandrasekhar mass limit when the WD explodes. In this work, we studied the C/O ratio for accreting CO WDs. Employing the stellar evolution code MESA, we simulated the accretion of He-rich material onto CO WDs with different initial WD masses and different mass accretion rates. We found that the C/O ratio varies for different cases. The C/O ratio of He-accreting CO WDs at explosion increases with a decreasing initial WD mass or a decreasing accretion rate. The various C/O ratios may, therefore, contribute to the diversity of SNe Ia.

Key words: stars: evolution — supernovae: general — white dwarfs

1 INTRODUCTION

Type Ia supernovae (SNe Ia) are of great importance in astrophysics. They have been successfully used as standardizable candles for measuring cosmological distances due to their high luminosity and remarkable uniformity, leading to the discovery of the accelerating expansion of the universe which is driven by dark energy (Riess et al. 1998; Perlmutter et al. 1999). Also, SNe Ia are important for the evolution of their host galaxies since many heavy elements can be produced during their explosions (Greggio & Renzini 1983; Matteucci & Greggio 1986; Rana 1991). Besides, they are accelerators of cosmic rays (e.g., Helder et al. 2009; Fang & Zhang 2012).

Hoyle & Fowler (1960) suggested that SNe Ia result from thermonuclear explosions of carbon-oxygen white d-

warfs (CO WDs) in close binaries. Once a CO WD increases its mass close to the Chandrasekhar mass limit, the carbon in the degenerate core is ignited, and the explosive carbon burning may destroy the WD, which explodes as an SN Ia (Nomoto et al. 1984). However, no progenitor system before SN Ia explosion has been conclusively identified (Wang 2018). Recently, many different kinds of progenitor models of SNe Ia have been proposed (see Wang & Han 2012 for a review), and the most favourable models are the single-degenerate (SD) model and the double-degenerate (DD) model. For the SD model, a CO WD accretes material from its non-degenerate companion, and the WD grows in mass till it is close to the Chandrasekhar mass limit and explodes as an SN Ia (Whelan & Iben 1973; Nomoto et al. 1984; Hachisu et al. 1996; Li & van den Heuvel 1997; Han & Podsiadlowski

2004; Wang et al. 2009; Meng et al. 2009; Hillman et al. 2016; Meng & Podsiadlowski 2017). For the DD model, an SN Ia arises from the coalescence of two CO WDs due to angular momentum loss via gravitational wave radiation and explosion might happen if the combined mass of the merger is larger than the Chandrasekhar mass limit (Sparks & Stecher 1974; Iben & Tutukov 1984; Webbink 1984; Han 1998; Chen et al. 2012).

When SNe Ia are applied as distance indicators, the Phillips relation (Phillips 1993) is adopted. However, there exists spectroscopic diversity among SNe Ia that is presently not well understood; how this diversity is linked to the properties of their progenitors is also unclear (Branch et al. 1995; Wang & Han 2012). Arnett (1982) suggested that the amount of ^{56}Ni formed during a SN Ia explosion dominates its maximum luminosity. However, the origin of the variation in the amount of ^{56}Ni for different SNe Ia is still unclear (Podsiadlowski et al. 2008). It has been suggested that the ratio of carbon to oxygen (C/O) of a WD at the moment of SN explosion is the dominant parameter for the Phillips relation. That is to say, the higher the C/O ratio, the larger the amount of ^{56}Ni (Umeda et al. 1999a), and the higher the maximum luminosity. Meng et al. (2009) and Meng & Yang (2010) studied the initial masses of CO WDs in SN Ia progenitors with a binary population synthesis approach. They showed that the masses vary with population age and explained the brightness difference of SNe Ia between spiral galaxies and elliptical galaxies qualitatively when the C/O ratios (related to the initial masses of the CO WDs) dominate the amount of ^{56}Ni produced. Recently we have made detailed stellar evolution calculations for accreting CO WDs, and found that the C/O ratios for accreting WDs are higher than previously believed (Cui et al. 2018). However, the C/O ratios for accreting WDs at explosion are still not known. The ratios may influence the brightness and diversity of SNe Ia.

The purpose of this paper is to study the C/O ratios of He-accreting CO WDs at explosion in the SD model. Previous works have shown that the region of accretion rates for steady hydrogen shell burning is significantly lower than that for steady helium shell burning (Ma et al. 2013; Wang et al. 2015), and hydrogen-rich material accretion leads to helium shell flashes (Cui et al. 2018) as a result. Therefore it is unrealistic to do calculations that follow the accretion of H-rich material till explosion. In this paper, we use the stellar evolution code MESA to simulate the accreting process, letting WDs accrete He-rich material. We describe our primary method and simulation code

in Section 2, and present the results in Section 3. Finally, we discuss the results and conclude in Sections 4 and 5.

2 METHODS

We employ the stellar evolution code MESA (version5329) (Paxton et al. 2011, 2013, 2015, 2018) to simulate the accretion of He-rich material onto CO WDs. Two relevant MESA suite cases (make_co_wd and wd2) are used for our simulations. The suite case make_co_wd is used to create initial CO WD models. We can create different kinds of WDs ($Z = 0.02$) by using the suite case make_co_wd, and simulate the accretion of He-rich material ($Y = 0.98$, $Z = 0.02$) onto WDs by using the suite case wd2. The nuclear network consists of the isotopes needed for helium, carbon and oxygen burning, which are coupled with more than 50 nuclear reactions.

Wang et al. (2015) and Wang et al. (2017) have obtained the steady burning region for helium accretion onto CO WDs. We follow the work of Wang et al. (2015) and Wang et al. (2017), adopting their \dot{M}_{Edd} and \dot{M}_{stable} . Moreover, Wang et al. (2017) found a critical accretion rate above which off-centre carbon ignition occurs when the WD mass approaches the Chandrasekhar mass limit. Since we want to study the C/O ratio for the WD at the explosion of the SN Ia, the parameter space for WDs and accretion rates we use in our study can only be selected in the region where explosive carbon burning is shown by Wang et al. (2017) to occur. The initial WD masses are, therefore, chosen to be 0.8, 0.9, 1.0, and 1.1 M_{\odot} and the accretion rates are 1.4, 1.6, 1.8, and $2.0 \times 10^{-6} M_{\odot} \text{ yr}^{-1}$ in our simulations. We only select the initial parameters at which helium shell burning could be steady during the evolution so that the mass retention efficiency of helium shell burning is about 100%. However, it is difficult to determine the lower boundary of the steady burning region (Kato & Hachisu 2004; Piersanti et al. 2014; Wang et al. 2015, 2017). The WD may undergo several flashes before steady burning if the \dot{M}_{acc} is close to the lower boundary. Nevertheless, these flashes could hardly affect the results.

An accreting WD grows in mass via steady helium shell burning and finally approaches the Chandrasekhar mass limit. Carbon may be ignited in the centre, and the carbon burning can be explosive. To determine the starting point of explosive carbon ignition in the simulation, Lesaffre et al. (2006) suggested that SNe Ia explosion occurs when the accreting WD evolves to the point $t_{\text{b}} = 1/22 t_{\text{c}}$, where t_{b} is the exponential temperature growth time of carbon burning and t_{c} is a convective element crossing time over a pressure scale height. Chen

et al. (2014) and Wu et al. (2016), however, chose the point where the central temperature of the WD increases sharply, but the central density of the WD remains nearly the same. Such a choice is more physical, and the point is later than that of Lesaffre et al. (2006). In this work, we follow Chen et al. (2014) and Wu et al. (2016) in choosing the point for explosive carbon ignition.

3 RESULTS

In Figures 1–3, we present a representative case in our simulations, in which a WD with an initial mass of $1.0 M_{\odot}$ accretes He-rich material at a rate of $1.6 \times 10^{-6} M_{\odot} \text{ yr}^{-1}$. Figure 1 shows the mass, the luminosity, and the radius of the WD during the accretion. It demonstrates that the helium shell burns steadily as we expected, and the mass of the WD increases linearly with time. It is evident that helium shell burning converts He-rich material to carbon and oxygen. The radius of the WD decreases as mass increases, consistent with the mass-radius relation of WDs.

Figure 2 presents the evolution of central density and temperature for the accreting WD. We see that the density and the temperature increase first during the accretion. At the final stage of accretion, carbon starts to burn, the WD expands (the central density drops), and finally the central density remains nearly the same but the central temperature increases quickly, which leads to the rapid growth of the carbon burning rate at the centre. In our simulations, we choose the dot in Figure 2 as the starting point of explosive carbon burning, and it is later than what was used in Lesaffre et al. (2006) (the cross in Fig. 2).

We present the profiles of the mass fractions of helium, carbon, and oxygen of the WD at the moment just before explosion (i.e., before the explosive ignition point) in panels (a) and (b) of Figure 3. The accreted helium shell burns into carbon and oxygen, and this leads to the growth of the WD core. Similar to the results in Cui et al. (2018), the helium shell’s steady burning leads to a higher carbon mass fraction. Panel (c) shows the profiles of the elements and convection region at the exact moment of carbon explosion (i.e., at the explosive ignition point). We see the boundary of the convective core reaches about $1.2 M_{\odot}$. After testing different initial WD masses and accretion rates, we find that the boundary of the convective core remains the same.

Figure 4 shows the evolution of the carbon fraction for accreting WDs with initial masses of 0.9 and $1.0 M_{\odot}$ and different accretion rates. Here the carbon fraction is defined as the ratio of the total carbon mass to the total mass of the WD. We see that the carbon fraction becomes higher during accretion since helium shell burning results in a

higher carbon mass fraction than that of the initial WD. We also see that a higher accretion rate leads to a lower carbon fraction for a given WD. The reason is that the temperature of the helium shell burning region is different for various accretion rates. A higher accretion rate leads to a higher temperature, and a higher temperature leads to greater oxygen gain by helium burning. Moreover, the initial WD mass has a significant influence on the C/O ratio as a lower mass CO WD has a higher C/O ratio inherently.

At the moment of explosion, a convection region of $1.2 M_{\odot}$ is developed (see panel (c) of Fig. 3), and the explosive ignition is at the centre. We define the carbon fraction in the convection region of the WDs at the moment of explosion as the ratio of the total carbon mass in the region to the total mass in the region. In Figure 5, we present the carbon fractions of the WDs and the carbon fractions in the convection regions at the moment of explosion for a range of initial WD masses and different accretion rates. We find that the carbon fractions and hence the C/O ratios¹ increase with either a decreasing initial WD mass or a decreasing accretion rate.

4 DISCUSSION

In this work, we investigate the C/O ratio of CO WDs during the process of helium accretion. By adopting the accretion rates of Wang et al. (2015, 2017) for steady helium shell burning, we simulate the accretion of He-rich material onto WDs. We find that the C/O ratio changes with different initial WD masses and different accretion rates. In particular, both a lower initial WD mass and a lower accretion rate result in a higher C/O ratio.

A low mass CO WD tends to result from a low mass AGB star, and this will lead to a higher initial C/O ratio of the WD. Similarly, a lower accretion rate leads to a higher C/O ratio. The reason is that the C/O ratio depends on the temperature and the density of the helium burning region. As an example, Figure 6 shows the temperature of the helium burning region for a $1.1 M_{\odot}$ WD under different accretion rates during its evolution. When helium burning starts, both 3α reaction for C production and 4α reaction for O production occur. The nuclear reaction rate for 4α reaction increases faster than that for 3α with the increase of temperature (Duorah & Kushwaha 1963). Consequently, a higher temperature for the helium burning region leads to more oxygen gained (i.e., a lower C/O ratio).

¹ Note the sum of the carbon fraction, the oxygen fraction, the helium fraction and Z of a WD at explosion or that in the convection region is 1.0, and the helium fraction is negligible. A higher carbon fraction means a higher C/O ratio.

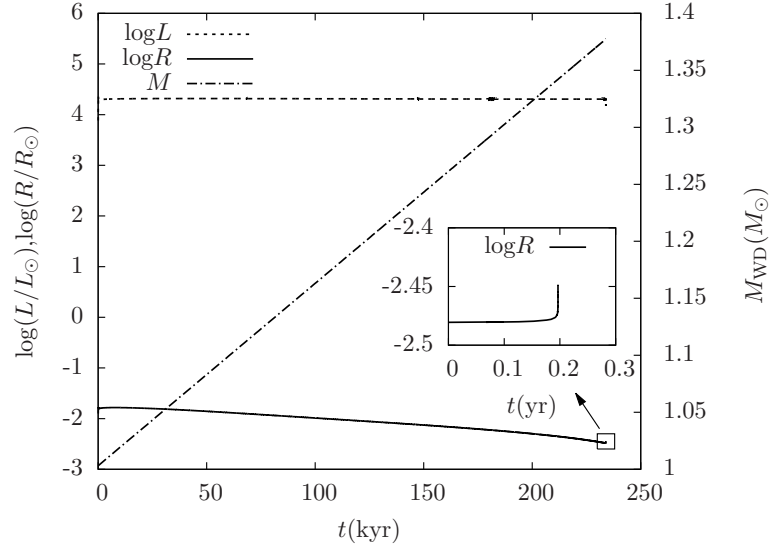


Fig. 1 The mass, luminosity and radius during accretion of He-rich material for a WD with an initial mass of $1.0 M_{\odot}$ and an accretion rate of $1.6 \times 10^{-6} M_{\odot} \text{ yr}^{-1}$.

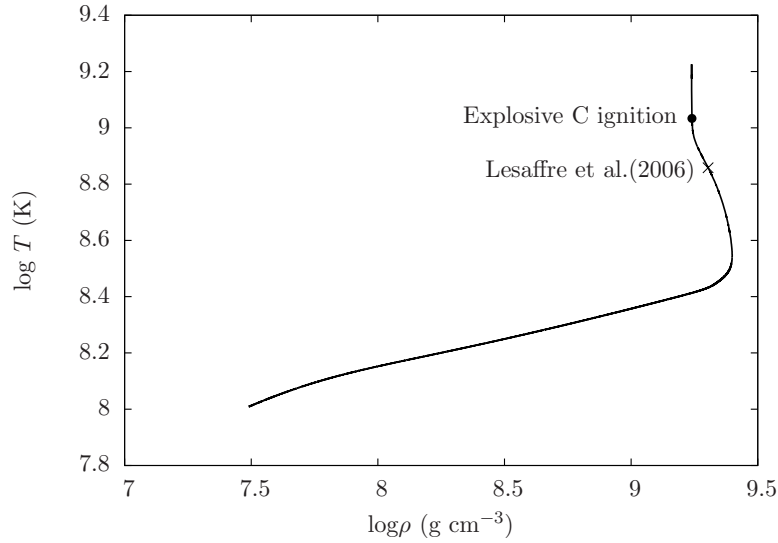


Fig. 2 The central density and central temperature during accretion of He-rich material for a WD with an initial mass of $1 M_{\odot}$. The *dot* represents the starting point for explosive carbon burning we use, while the *cross* shows the point of Lesaffre et al. (2006).

We only simulate the steady burning region of He-accreting CO WDs. But if the accretion rate is relatively low, the helium shell would flash and the mass retention efficiency of the WD would be low. Therefore, the C/O ratio for WDs may be different from that of steady burning. We make a comparison in Figure 7 for a sample of a $1.0 M_{\odot}$ WD at a low accretion rate ($0.9 \times 10^{-6} M_{\odot} \text{ yr}^{-1}$). Since the calculation of helium shell flashes is difficult and consume too much cpu time, we only increase the WD mass to about $1.05 M_{\odot}$. We can see that if the accretion rate is

lower than that of the steady burning region, the C/O ratio would be lower because of the flash.

In our simulation, we do not consider the rotation of the WDs. If rotation is taken into account, the WD mass may exceed the Chandrasekhar mass limit (see Yoon & Langer 2004; Hachisu et al. 2012; Wang et al. 2014). This could lead to more helium shell burning and the burning region would have a lower temperature. We would, therefore, expect a higher final C/O ratio.

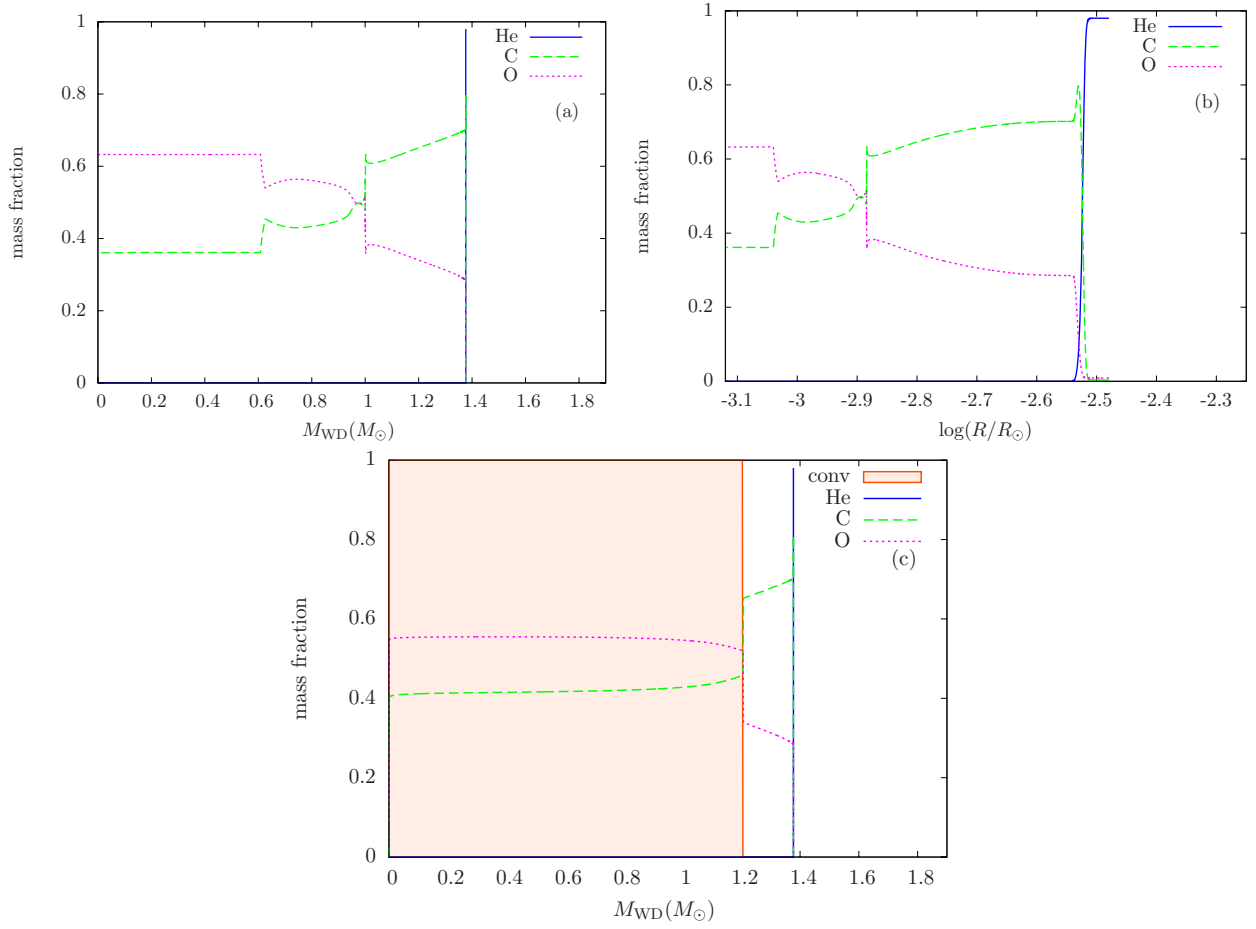


Fig. 3 The chemical profile of the accreting WD just before explosion (panels a, b) and at the moment of explosion (c). The *filled area* is for the convective region.

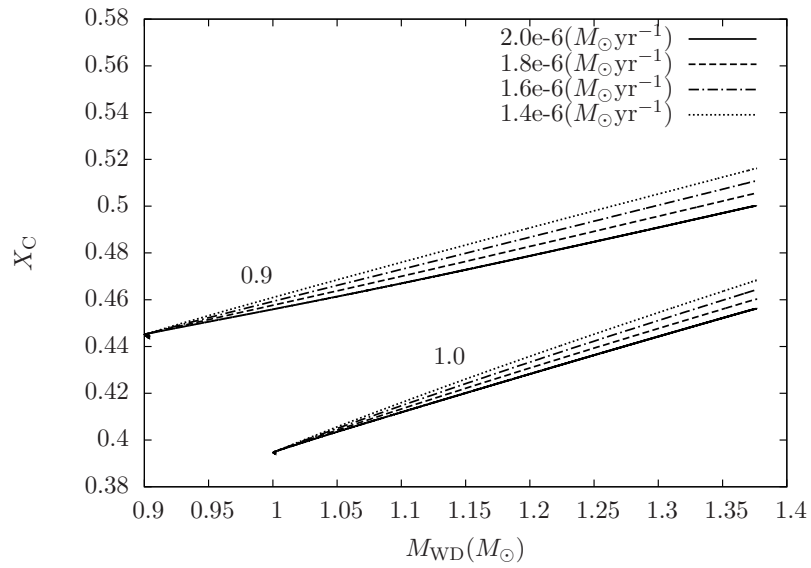


Fig. 4 The carbon fraction for accreting WDs with initial masses of $0.9 M_{\odot}$ and $1.0 M_{\odot}$. The different line types represent different accretion rates.

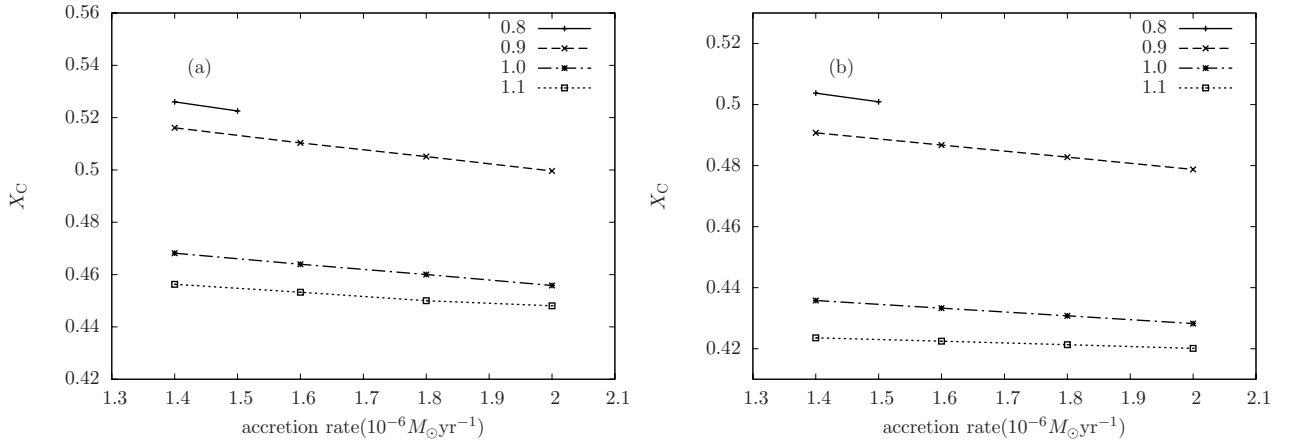


Fig. 5 The carbon fraction of the WDs (a) and the fraction in the convective regions (b) at the moment of explosion. The different lines stand for different initial WD masses.

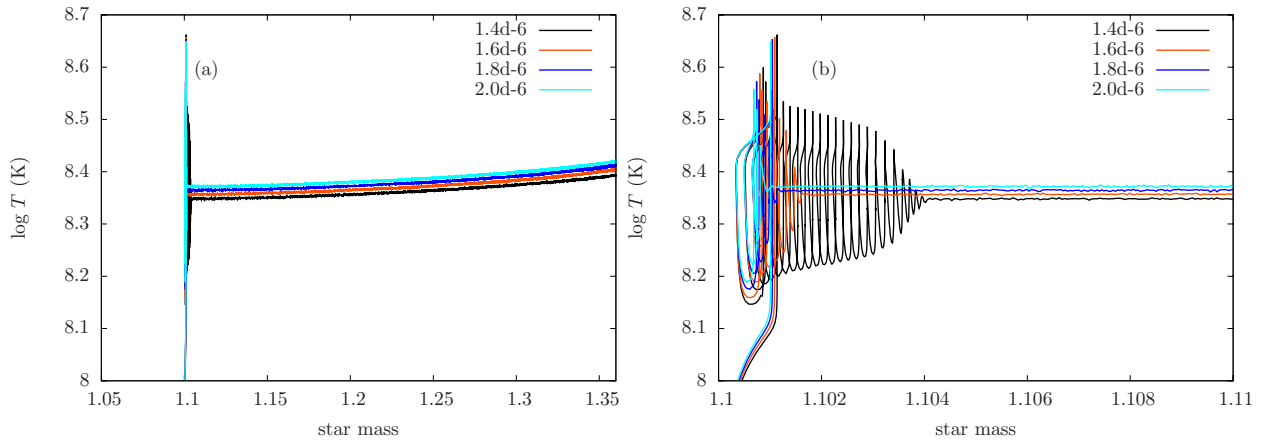


Fig. 6 The temperature of the helium burning region for a $1.1 M_{\odot}$ WD with different accretion rates during the evolution. Panel (b) shows the details at the beginning of the evolution; the helium may undergo several flashes before steady burning especially for the lower accretion rate.

For the standard SD model, a WD can also accrete H-rich matter from its non-degenerate donor. In this case, H-rich material is accreted onto a CO WD and the resulting hydrogen burning shell converts hydrogen to helium. The resulting helium shell underneath the hydrogen shell burns helium into carbon and oxygen, leading to the growth of the CO WD (Cui et al. 2018). Previous works have shown that the steady burning region for hydrogen is much lower than that of helium burning (e.g., Nomoto et al. 1984; Hachisu et al. 1996; Ma et al. 2013; Wang et al. 2015; Piersanti et al. 2014; Hillman et al. 2016). The C/O ratio for WDs accreting H-rich material may be different from that of WDs accreting He-rich material. The accretion is more complicated because of helium shell flashes.

It has been suggested that the C/O ratio of a WD at the moment of the explosion may affect the amount of ^{56}Ni formed during an SN Ia (Umeda et al. 1999a). Since the amount of ^{56}Ni formed during an SN Ia explosion dom-

inates its maximum luminosity (Arnett 1982), a higher C/O ratio for the CO WD at explosion may lead to more ^{56}Ni formed and make the resulting SN Ia more luminous. Previous works have usually used a low C/O ratio resulting from central helium burning, and the C/O ratio at explosion is often assumed to be a particular value (Umeda et al. 1999b; Höflich et al. 2010; Meng & Yang 2011). However, our study shows that the C/O ratios could be quite diverse for WDs of different initial masses and different accretion rates, which should be taken into account in future studies.

5 CONCLUSIONS

Employing MESA, we have investigated the accretion process of He-rich material onto CO WDs. We use different initial WD masses (0.8, 0.9, 1.0, and $1.1 M_{\odot}$) and accretion rates ($1.4, 1.6, 1.8,$ and $2.0 \times 10^{-6} M_{\odot} \text{ yr}^{-1}$) in our simulations, and the results indicate that both a lower ini-

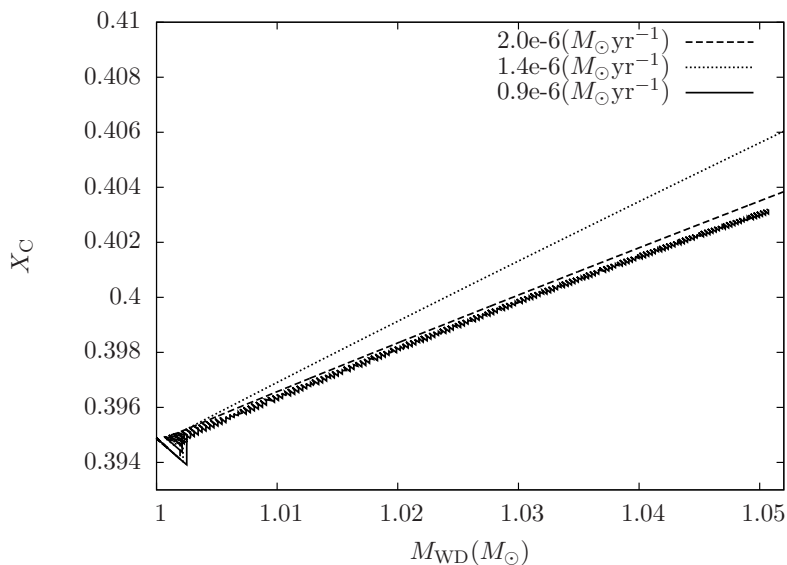


Fig. 7 Similar to Fig. 4, a comparison of carbon fractions for a $1.0 M_{\odot}$ WD with low accretion rates. The different line types represent different accretion rates. The accretion rate of $0.9 \times 10^{-6} M_{\odot} \text{ yr}^{-1}$ corresponds to the helium shell flash.

tial WD mass and a lower accretion rate result in a higher C/O ratio for accreting CO WDs before their explosion. These results can be used for future explosion simulations of SNe Ia. The variation of the C/O ratio of CO WDs at the moment of explosion may be one of the reasons for SN Ia diversity.

Acknowledgements We thank Dr. Hailiang Chen and Dr. Dongdong Liu for their useful discussions and suggestions. This study is partly supported by the National Natural Science Foundation of China (Grant Nos. 11521303, 11873085, 11673059 and 11733008), the Chinese Academy of Sciences (QYZDB-SSW-SYS001), and the Natural Science Foundation of Yunnan Province (2015HB096 and 2018FB005).

References

- Arnett, W. D. 1982, *ApJ*, 253, 785
- Branch, D., Livio, M., Yungelson, L. R., Boffi, F. R., & Baron, E. 1995, *PASP*, 107, 1019
- Chen, X., Jeffery, C. S., Zhang, X., & Han, Z. 2012, *ApJ*, 755, L9
- Chen, X., Han, Z., & Meng, X. 2014, *MNRAS*, 438, 3358
- Cui, X., Meng, X.-C., & Han, Z.-W. 2018, *RAA (Research in Astronomy and Astrophysics)*, 18, 058
- Duorah, H. L., & Kushwaha, R. S. 1963, *ApJ*, 137, 566
- Fang, J., & Zhang, L. 2012, *MNRAS*, 424, 2811
- Greggio, L., & Renzini, A. 1983, *A&A*, 118, 217
- Hachisu, I., Kato, M., & Nomoto, K. 1996, *ApJ*, 470, L97
- Hachisu, I., Kato, M., Saio, H., & Nomoto, K. 2012, *ApJ*, 744, 69
- Han, Z. 1998, *MNRAS*, 296, 1019
- Han, Z., & Podsiadlowski, P. 2004, *MNRAS*, 350, 1301
- Helder, E. A., Vink, J., Bassa, C. G., et al. 2009, *Science*, 325, 719
- Hillman, Y., Prialnik, D., Kovetz, A., & Shara, M. M. 2016, *ApJ*, 819, 168
- Höflich, P., Krisciunas, K., Khokhlov, A. M., et al. 2010, *ApJ*, 710, 444
- Hoyle, F., & Fowler, W. A. 1960, *ApJ*, 132, 565
- Iben, Jr., I., & Tutukov, A. V. 1984, *ApJS*, 54, 335
- Kato, M., & Hachisu, I. 2004, *ApJ*, 613, L129
- Lesaffre, P., Han, Z., Tout, C. A., Podsiadlowski, P., & Martin, R. G. 2006, *MNRAS*, 368, 187
- Li, X.-D., & van den Heuvel, E. P. J. 1997, *A&A*, 322, L9
- Ma, X., Chen, X., Chen, H.-l., Denissenkov, P. A., & Han, Z. 2013, *ApJ*, 778, L32
- Matteucci, F., & Greggio, L. 1986, *A&A*, 154, 279
- Meng, X., Chen, X., & Han, Z. 2009, *MNRAS*, 395, 2103
- Meng, X., & Yang, W. 2010, *ApJ*, 710, 1310
- Meng, X. C., & Yang, W. M. 2011, *A&A*, 531, A94
- Meng, X., & Podsiadlowski, P. 2017, *MNRAS*, 469, 4763
- Nomoto, K., Thielemann, F.-K., & Yokoi, K. 1984, *ApJ*, 286, 644
- Paxton, B., Bildsten, L., Dotter, A., et al. 2011, *ApJS*, 192, 3
- Paxton, B., Cantiello, M., Arras, P., et al. 2013, *ApJS*, 208, 4
- Paxton, B., Marchant, P., Schwab, J., et al. 2015, *ApJS*, 220, 15
- Paxton, B., Schwab, J., Bauer, E. B., et al. 2018, *ApJS*, 234, 34
- Perlmutter, S., Aldering, G., Goldhaber, G., et al. 1999, *ApJ*, 517, 565
- Phillips, M. M. 1993, *ApJ*, 413, L105
- Piersanti, L., Tornambé, A., & Yungelson, L. R. 2014, *MNRAS*, 445, 3239
- Podsiadlowski, P., Mazzali, P., Lesaffre, P., Han, Z., & Förster, F.

- 2008, *New Astron. Rev.*, 52, 381
- Rana, N. C. 1991, *ARA&A*, 29, 129
- Riess, A. G., Filippenko, A. V., Challis, P., et al. 1998, *AJ*, 116, 1009
- Sparks, W. M., & Stecher, T. P. 1974, *ApJ*, 188, 149
- Umeda, H., Nomoto, K., Kobayashi, C., Hachisu, I., & Kato, M. 1999a, *ApJ*, 522, L43
- Umeda, H., Nomoto, K., Yamaoka, H., & Wanajo, S. 1999b, *ApJ*, 513, 861
- Wang, B. 2018, *RAA (Research in Astronomy and Astrophysics)*, 18, 049
- Wang, B., Meng, X., Chen, X., & Han, Z. 2009, *MNRAS*, 395, 847
- Wang, B., & Han, Z. 2012, *New Astron. Rev.*, 56, 122
- Wang, B., Justham, S., Liu, Z.-W., et al. 2014, *MNRAS*, 445, 2340
- Wang, B., Li, Y., Ma, X., et al. 2015, *A&A*, 584, A37
- Wang, B., Podsiadlowski, P., & Han, Z. 2017, *MNRAS*, 472, 1593
- Webbink, R. F. 1984, *ApJ*, 277, 355
- Whelan, J., & Iben, Jr., I. 1973, *ApJ*, 186, 1007
- Wu, C.-Y., Liu, D.-D., Zhou, W.-H., & Wang, B. 2016, *RAA (Research in Astronomy and Astrophysics)*, 16, 160
- Yoon, S.-C., & Langer, N. 2004, *A&A*, 419, 623